doi:10.1016/j.jmb.2008.03.054 J. Mol. Biol. (2008) 380, 83–94

JMB

Available online at www.sciencedirect.com

ScienceDirect

ELSEVIER

A Betacellulin Mutant Promotes Differentiation of Pancreatic Acinar AR42J Cells into Insulin-Producing Cells with Low Affinity of Binding to ErbB1

Tadahiro Nagaoka[1], Takayuki Fukuda[1], Toshihiro Hashizume[1], Tomoko Nishiyama[1], Hiroko Tada[1], Hidenori Yamada[1], David S. Salomon[2], Satoko Yamada[3], Itaru Kojima[3] and Masaharu Seno[1]*

[1]*Department of Medical Bioengineering, Graduate School of Natural Science and Technology, Okayama University, 3-1-1 Tsushima-Naka, Okayama 700-8530, Japan*

[2]*Mammary Biology and Tumorigenesis Laboratory, National Cancer Institute, Bethesda, MD 20892, USA*

[3]*Institute for Molecular and Cellular Regulation, Gunma University, 3-39-15 Showamachi, Maebashi 371-8512, Japan*

Received 9 November 2007; received in revised form 10 March 2008; accepted 25 March 2008
Available online 3 April 2008

Edited by M. Seno

Betacellulin (BTC) is one of the members of the epidermal growth factor (EGF) ligand family of ErbB receptor tyrosine kinases. It is a differentiation factor as well as a potent mitogen. BTC promotes the differentiation of pancreatic acinar-derived AR42J cells into insulin-producing cells. It independently and preferentially binds to two type I tyrosine kinase receptors, the EGF receptor (ErbB1) and ErbB4. However, the physiochemical characteristics of BTC that are responsible for its preferential binding to these two receptors have not been fully defined. In this study, to investigate the essential amino acid residues of BTC for binding to the two receptors, we introduced point mutations into the EGF domain of BTC employing error-prone PCR. The receptor binding abilities of 190 mutants expressed in *Escherichia coli* were assessed by enzyme immunoassay. Replacement of the glutamic acid residue at position 88 with a lysine residue in BTC was found to produce a significant loss of affinity for binding to ErbB1, while the affinity of binding to ErbB4 was unchanged. In addition, the mutant of BTC-E/88/K showed less growth-promoting activity on BALB/c 3T3 cells compared with that of the wild-type BTC protein. Interestingly, the BTC mutant protein promoted differentiation of pancreatic acinar AR42J cells at a high frequency into insulin-producing cells compared with AR42J cells that were treated with wild-type BTC protein. These results indicate the possibility of designing BTC mutants, which have an activity of inducing differentiation only, without facilitating growth promotion.

Keywords: betacellulin; ErbB1; ErbB4; receptor–ligand interaction; cell differentiation

**Corresponding author.* E-mail address: mseno@cc.okayama-u.ac.jp.

Present address: T. Nagaoka, Mammary Biology and Tumorigenesis Laboratory, National Cancer Institute, Bethesda, MD 20892, USA.

Abbreviations used: BTC, betacellulin; EGF, epidermal growth factor; TGF, transforming growth factor; BTC-mut, BTC mutant; sErbB, soluble ErbB; ECD, extracellular domain; IgG, immunoglobulin G; HF, hinge–FLAG; EIA, enzyme immunoassay; HA, hemagglutinin; rhBTC, recombinant human BTC; MTT, 3-(4,5-dimetylthiazol-2-yl)-2,5-diphenyl tetrazolium bromide; PBS, phosphate-buffered saline; BSA, bovine serum albumin; PBS-T, phosphate-buffered saline with 0.1% Tween-20.

Introduction

Betacellulin (BTC) is a member of the epidermal growth factor (EGF) family of proteins that was originally isolated from the conditioned medium of β-TC-3 insulinoma cells.[1] It is predominantly expressed in the adult pancreas, small intestine, kidney and liver and at lower levels in the heart, lung and skeletal muscle.[2,3] BTC is expressed as a membrane-bound precursor composed of 178 amino acid residues. The metalloprotease ADAM10 mediates ectodomain shedding of the BTC precursor to generate an 80-amino-acid mature BTC protein. The soluble form of human BTC has been recombinantly pre-

0022-2836/$ - see front matter

pared from *Escherichia coli* and biologically characterized.[3–5] It is known that BTC binds and activates both the ErbB1 and ErbB4 type I tyrosine kinase receptors.[5,6] BTC promotes proliferation of fibroblasts, smooth muscle and epithelial cells to a similar extent as EGF and transforming growth factor-α (TGF-α).[2] It also induces the differentiation of amylase-secreting rat pancreatic AR42J acinar cells into insulin-secreting cells *in vitro*.[7] This activity is unique to BTC among members of the EGF ligand family. In addition, activin A, a member of the TGF-β superfamily, can enhance the differentiation activity of BTC. BTC can also promote pancreatic β-cell regeneration *in vivo* in either rats or mice, in which pancreatic β cells were destroyed with streptozotocin or removed by pancreatectomy.[8–10] From these observations, BTC might be applicable for regeneration therapy of pancreatic β cells and for the treatment of diabetes. However, the mitogenic activity of BTC might induce growth of potential pancreatic tumors. We therefore ascertained if we would construct a BTC variant that would facilitate pancreatic differentiation but which would not stimulate proliferation.

The amino acid residues of EGF and TGF-α that are involved in the binding of these peptides to ErbB1 were previously investigated by site-directed mutagenesis.[11–13] Simultaneously, those responsible for binding to ErbB3 and ErbB4 in the EGF domain of heregulin-β were studied by alanine scanning mutagenesis.[14] However, no relationship between receptor binding specificity and biological activity has been reported.

In this work, we describe a procedure for random mutagenesis, so-called error-prone PCR, to create BTC mutants (BTC-muts) and for the preparation of soluble ErbB (sErbB) receptors consisting of the extracellular domains (ECDs) fused to the immunoglobulin G (IgG) hinge region, which enables for screening of altered affinity of BTC binding to either ErbB1 or ErbB4. As a result, we could successfully identify the essential amino acid residues of BTC that are responsible for controlling the affinity of binding of BTC to ErbB1 and ErbB4.

Results

Generation of dimeric forms of sErbB1 and sErbB4 fused to the hinge region of the mouse immunoglobulin gamma chain

We designed and prepared a novel type of sErbB receptors consisting of the ectodomains of ErbB1 and ErbB4 to detect the binding of BTC *in vitro*. A number of soluble receptors have been designed as Fc fusion proteins have previously been constructed.[15,16] One of the advantages of Fc fusion proteins is the efficient formation of stable homodimers of target proteins. However, the molecular weights of Fc-fused sErbB receptors are large (~300,000) and it is difficult to distinguish dimers from oligomers after resolution on SDS-PAGE. The ECD of ErbB1, even without the transmembrane and cytoplasmic regions, has the potential to homodimerize when bound to EGF.[17] These points led us to design homodimeric forms of sErbB1 and sErbB4 that are fusion proteins between each ECD and the hinge region of mouse IgG–Fc, which is responsible for heavy chain dimerization of immunoglobulin molecules (Fig. 1a). For detection in Western blotting, the hinge region was coupled to a FLAG tag at the C-terminus. Both sErbB1–hinge–FLAG (sErbB1-HF) and sErbB4–hinge–FLAG (sErbB4-HF) expression vectors were transfected into 293-H cells, and stable transformants expressing sErbB-HF were obtained by G418 selection. The recombinant proteins that were secreted into the culture media were confirmed by immunoprecipitation with an anti-FLAG antibody conjugated to agarose. SDS-PAGE under reducing or non-reducing conditions revealed that dimerization was detected only when the hinge region was fused to sErbBs and not without the hinge region (Fig. 1b). The ratio of monomeric and oligomeric forms was densitometrically measured and calculated (Table 1). Without the hinge region, sErbB1–FLAG (sErbB1-F) and sErbB4–FLAG (sErbB4-F) were detected as monomeric forms at frequencies of 74% and 63%, respectively. The sErbBs fused to the hinge region, sErbB1-HF and sErbB4-HF, existed as dimeric forms at frequencies of 89% and 95%, respectively.

The binding affinity of BTC for both the sErbB1-HF and sErbB4-HF forms was assessed by a competitive enzyme immunoassay (EIA) exploiting BTC fused to a hemagglutinin (HA)–myc–His epitope tag, His–myc–BTC–HA. The dissociation constant (K_d) between sErbB1-HF and BTC was estimated to be 0.35 nM. This K_d was calculated with the use of the Scatchard analysis (Fig. 1c) and was consistent with the K_d that was previously reported for BTC binding to ErbB1.[5] In addition, sErbB1-HF might possess a high-affinity binding site of BTC because we observed a few points on the Scatchard plot that were separated from the regression line. As for sErbB4-HF, the K_d of BTC binding was estimated to be 3.2 nM, which was 10-fold lower than the binding affinity of BTC to ErbB1. This is the first report that has assessed a K_d between BTC and dimerized ECD of ErbB4. This K_d value is consistent with a report that described an affinity of ErbB4 to BTC as slightly weaker than that of ErbB1 to BTC.[16] These results indicate that our sErbB-HFs retained the ability to bind to BTC, as well as the binding to membrane-associated ErbB receptors.

BTC-mut proteins and their affinity for ErbB1 and ErbB4 binding

The EGF motif is highly conserved among the members of the EGF family of peptides. Since replacement of amino acid residues could change the receptor binding ability of BTC, we designed a mutant library composed of mutants with one or two mutations in the amino acid sequence. We first examined the reaction conditions of error-prone PCR changing the concentration of manganese (II) from 0 to 50 μM in the presence of deoxy-ITP. The resultant DNA frag-

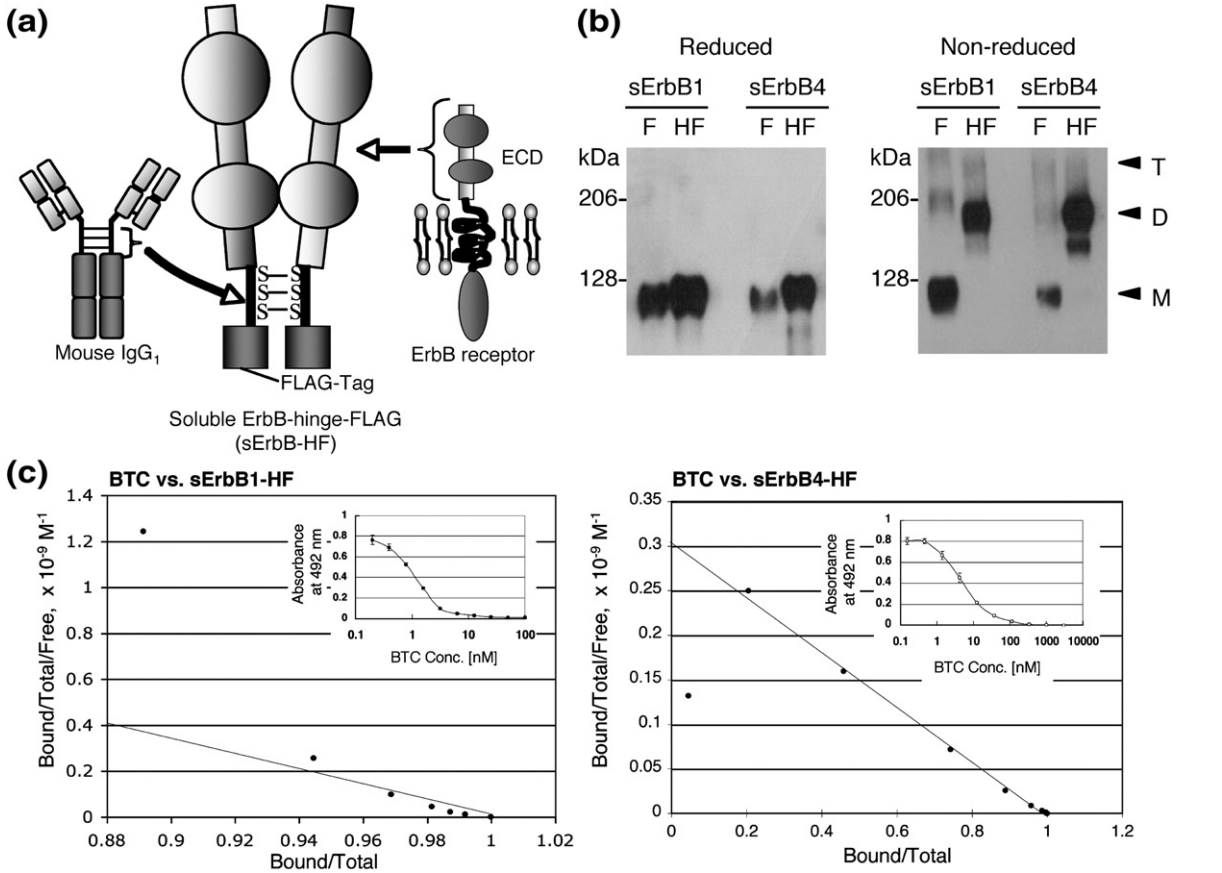

Fig. 1. The schematic design of sErbB dimer fused to the IgG hinge region. (a) The hinge region was fused to the C-terminus of the ECD of ErbBs for dimerization through disulfide links. The FLAG tag was fused to the C-terminus of the hinge region for easy detection by anti-FLAG antibody. (b) The ECDs of ErbB1 and ErbB4 fused to FLAG (F) or to both hinge and FLAG (HF) were expressed in 293-H cells and immunoprecipitated from the conditioned media by anti-FLAG agarose and immunoblotted by biotin-labeled anti-FLAG antibody. SDS-PAGE was carried out under reduced or non-reduced conditions. M, monomer; D, dimer; T, trimer. (c) Evaluation of the affinity of sErbB-HF to BTC. K_d values of sErbB-HFs and BTC were calculated from the Scatchard plots based on the competitive EIA.

ment was used as the primer set to produce the full length of BTC expression plasmid. The BTC expression plasmid DNA was transfected to *E. coli*; five clones of the transformants were obtained from each condition and were randomly picked; and plasmid DNA was extracted and sequenced for the EGF motif. As the concentration of manganese (II) increased, the mutation of nucleotides increased (Fig. 2). When error-prone PCR was carried out in 10 μM $MnCl_2$, the mutants showed 3.6±1.5 nucleotide mutations per 141 bp (2.0±0.9 mutations per 47 amino acid residues). We therefore employed this condition

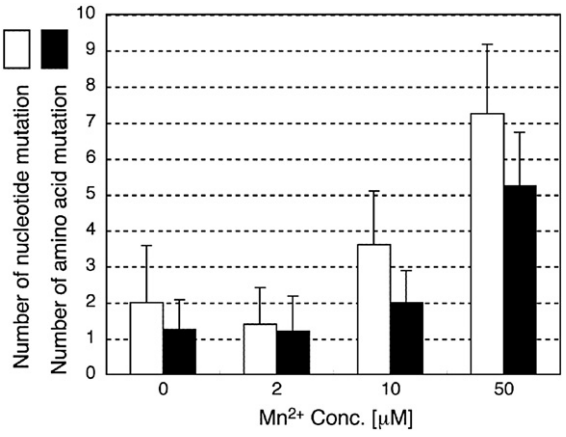

Fig. 2. Frequency of mutations in the EGF motif of BTC by error-prone PCR depending on Mn^{2+} concentration. Error-prone PCR was carried out in varying concentrations of $MnCl_2$ to introduce random mutation into the EGF motif of BTC. Five clones were picked up in each reaction condition, and mutations were determined by DNA sequencing. The white bar indicates the number of nucleotide mutations per 141 bp, while the black bar indicates the number of amino acid mutations due to the nucleotide mutations per 47 amino acids.

Table 1. Ratio of oligomeric forms of soluble receptors detected in SDS-PAGE without reducing reagents[a]

	sErbB1-F	sErbB1-HF	sErbB4-F	sErbB4-HF
Monomer	74.0	0	62.6	0.9
Dimer	17.6	88.9	26.8	94.6
Trimer	8.4	11.1	10.6	4.5

Data are expressed as percentages.
[a] Results are summarized from the SDS-PAGE in Fig. 1b.

of error-prone PCR with 10 μM $MnCl_2$, which would optimize the mutation rate, resulting in the replacement of at least one amino acid residue in BTC. The PCR products were used to transform *E. coli* BL21-Gold(DE3) pLysS to obtain clones grown in the presence of 100 μg/ml of ampicillin and 15 μg/ml of chloramphenicol. The resultant 190 colonies were cultured independently in 96-deep-well plates, and mutant proteins were expressed. The crude extracts including each BTC-mut were collected. Seventeen BTC-muts were randomly selected from the plates and immunoblotted with an anti-HA antibody to confirm the presence of each mutant (Fig. 3a). The affinity of the BTC-muts in the crude extracts for ErbB1 and ErbB4 was evaluated with sErbB1-HF and sErbB4-HF in an EIA system. From the results, interaction indices were plotted to evaluate the preference of each BTC-mut for binding to ErbB1 or ErbB4 (Fig. 3b). Several mutants were picked according to the indices and evaluated in a secondary EIA. Mutants were found to segregate into three representative groups of clones 1C11, 2H6 and 2G10, of which DNA sequences corresponding to the EGF domain were validated. Two of the three mutants derived from clones 1C11 and 2H6 were found to have a mutation at the same amino acid residue. The mutations resulted in the replacement of the amino acid residue of D/108/G in 1C11 and 2H6 and that of E/88/K in 2G10 (Fig. 3c). These two BTC-muts were purified by Ni-chelating affinity chromatography, coated on the ELISA plates and then assessed for their binding affinity to ErbB1 and ErbB4 by competition EIA. Wild-type BTC (BTC-WT) or BTC-D/108/G derived from 1C11 coated in the ELISA plates was treated with a mixture of 2.7 nM sErbB1-HF and various concentrations of recombinant human BTC (rhBTC) to evaluate the binding affinity to ErbB1; in addition, BTC-E/88/K derived from 2G10-coated plates was treated with a mixture of 270 nM sErbB1-HF and various concentrations of rhBTC. Similarly, plates that were coated with BTC-WT or the two BTC-mut proteins were treated with a mixture of 2.7 nM sErbB4-HF and various concentrations of rhBTC to evaluate the binding affinity to ErbB4. Interaction between sErbB-HFs and the BTC proteins that were fixed on the plates was detected by addition of an anti-FLAG monoclonal antibody conjugated to peroxidase. As shown in Fig. 4, Scatchard plots evaluated for K_d values for BTC-mut proteins and binding to sErbB-HFs were estimated from the slope of the regression lines. Interestingly, BTC-E/88/K exhibited a 160-fold lower affinity for binding to ErbB1 compared with BTC-WT. In contrast, the affinities of binding to ErbB4 of both proteins were not significantly different (Table 2). In addition, the affinity of BTC-D/108/G for binding to either ErbB1 or ErbB4 was not significantly altered.

Mitogenic and differentiating activities of BTC-E/88/K mutant protein

The biological activity of the BTC-mut proteins was assessed by the growth promotion of BALB/c 3T3 cells and the differentiation of AR42J cells. Using

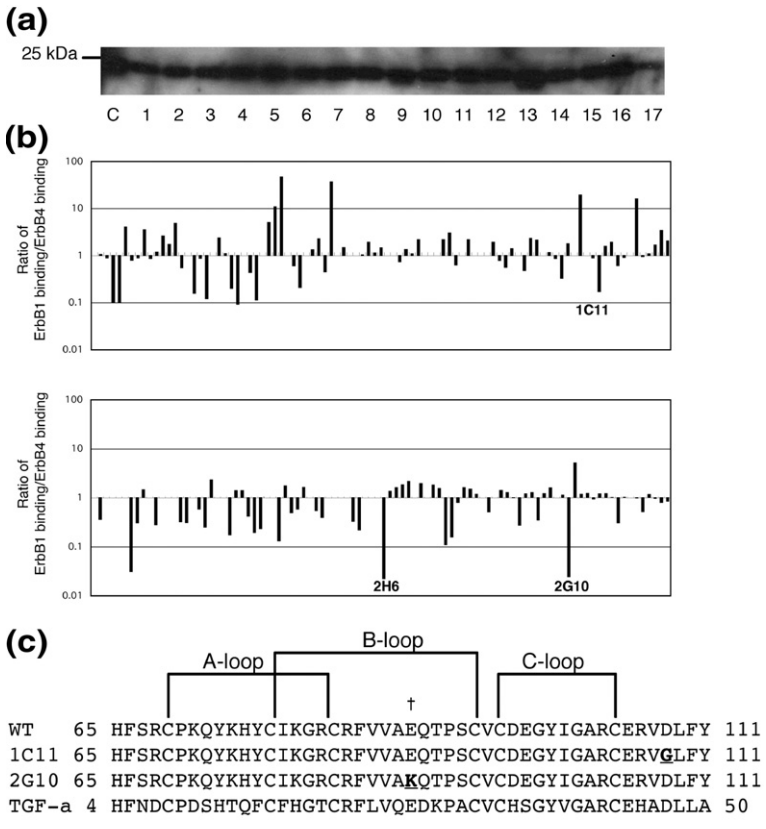

Fig. 3. Analyses of the mutants obtained by prone PCR. (a) Extracts from randomly selected 17 clones were checked for protein expression by Western blotting with anti-HA antibody. (b) Indices of binding specificity to ErbB1 and ErbB4 were evaluated from sErbB1/sErbB4 based on EIA. The sErbB1/sErbB4 value obtained from EIA of BTC-WT is taken as 1. The typical three mutants are indicated by their clone names. (c) Amino acid sequence alignment of the two types of clones and BTC-WT. Amino acid residues replaced by the mutation in the EGF motif are depicted with in boldface. The dagger indicates the mutation position of clone 2G10 (BTC-E/88/K). The positions of the cysteine residues are shown with the disulfide bridge pairs as A-, B- and C-loops.

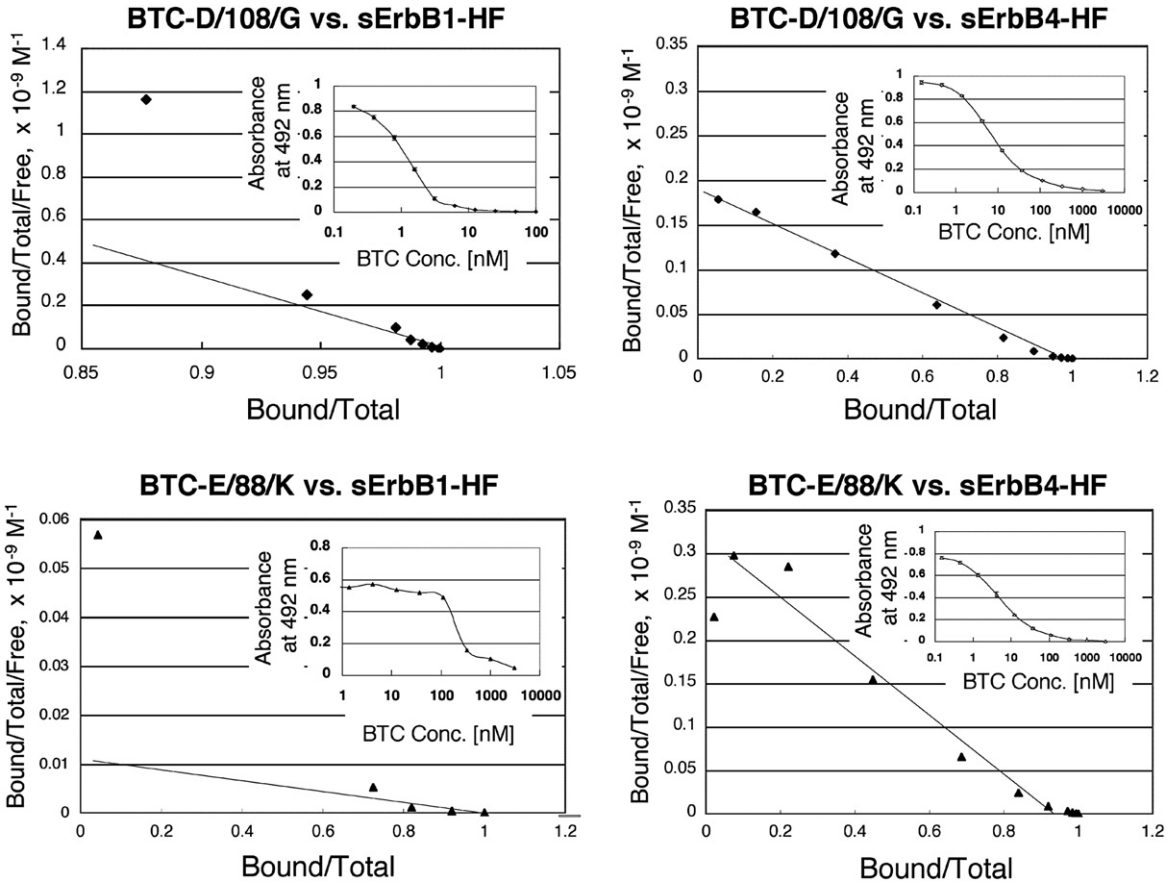

Fig. 4. Evaluation of the affinity of BTC-mut proteins for ErbB1 and ErbB4. BTC-E/88/K from the clone 2G10 and BTC-D/108/G from the clone 1C11 have been subjected to competitive EIA. K_d values of BTC-mut proteins and receptor were calculated from the Scatchard plots based on the competitive EIA. The K_d values are summarized in Table 2.

3-(4,5-dimetylthiazol-2-yl)-2,5-diphenyl tetrazolium bromide (MTT) assay to monitor cell proliferation, we observed an EC_{50} of 20 pM for BTC-WT protein in the ability to stimulate BALB/c 3T3 proliferation after 2 days. This EC_{50} value for BTC-WT protein was almost 30-fold lower than the concentration at which BTC–E/88/K protein produced a similar level of growth promotion (Fig. 5). This result indicates that the BTC-E/88/K protein has diminished activity to stimulate cell growth due to the looser affinity of binding to the ErbB1 compared with the BTC-WT protein.

Since BTC promotes differentiation of AR42J cells into insulin-expressing cells in the presence of activin A, the BTC-muts were assessed for activity in this context. AR42J cells were treated with BTC-WT or BTC-mut protein for 2 days in the presence of 2 nM activin A and were then evaluated for insulin expression by immunohistochemistry using an anti-insulin antibody (Fig. 6a). When AR42J cells were treated with 1 nM BTC-E/88/K mutant protein, insulin-positive cells appeared more frequently compared with

Table 2. Dissociation constant (K_d) values for BTC-muts and receptors

BTC	Mutation site	K_d for ErbB1 (nM)	K_d for ErbB4 (nM)
WT	—	0.35	3.2
1C11	D/108/G	0.19	5.1
2G10	E/88/K	58	6.7

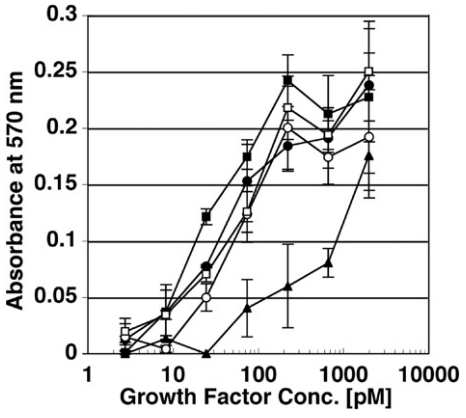

Fig. 5. Evaluation of cell growth-promoting activity of BTC and the mutant proteins. Two thousand BALB/c 3T3 A31 cells were cultured with the growth factors for 2 days. MTT was added to the culture medium, followed by incubation for 6 h at 37 °C to form MTT formazan. MTT formazan was dissolved with 10% SDS containing 20 mM HCl, and absorbance at 570 nm was measured. Closed square indicates EGF; closed circle, rhBTC; open circle, His–myc–BTC–HA; open square, BTC-D/108/G; and closed triangle, BTC-E/88/K. BTC-D/108/G was derived from 1C11.

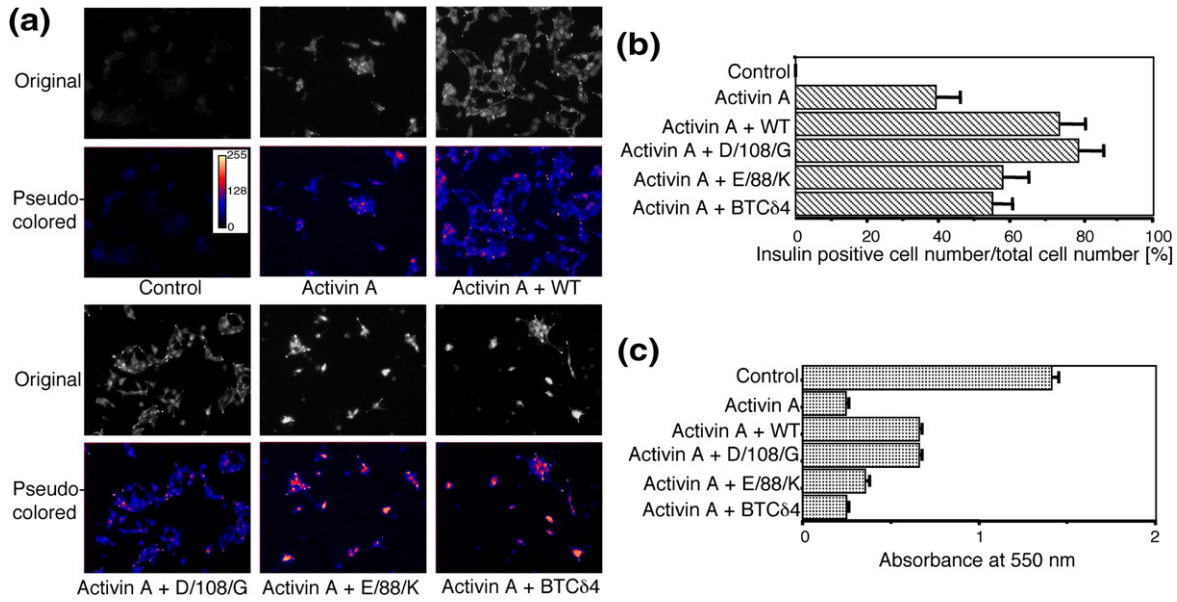

Fig. 6. Evaluation of the differentiation in AR42J cells. Insulin production in AR42J cells induced by BTC and its derivatives was assessed in the presence of activin A. (a) Cells were treated with BTC-muts in the presence of activin A and stained with anti-insulin antibody. Photographs of gray images (top) were shown as the fluorescent intensity with pseudocoloring function of "LUT_panel" plugin by using ImageJ. (b) The number of insulin-positive cells was counted in 5–10 fields in a 20×20-mm area, and the ratios of insulin-positive cells to all cells were plotted. (c) Cell proliferation was monitored by MTT assay. MTT formazan formed in the cells was dissolved, and absorbance at 550 nm was measured. SD was calculated from four independent experiments.

those treated with activin A only. This differentiation activity as assessed on AR42J cells by BTC-E/88/K was nearly equivalent in activity to that of BTC-WT protein (Fig. 6b). Sixty percent of the cells were induced to produce insulin when stimulated by BTC-E/88/K, while 70% of the AR42J cells were induced to produce insulin by BTC-WT protein. The BTC-E/88/K protein did not rescue the cell growth inhibition of AR42J cells that was produced by activin A (Fig. 6c). The intensity of fluorescence using an anti-insulin antibody showed that AR42J cells treated with BTC-E/88/K and activin A produced more insulin compared with those treated with BTC-WT and activin A (Fig. 6a). The BTC-E/88/K protein induced insulin production in AR42J cells similar to the BTC-δ4 protein, which lacks both C-loop in the EGF motif and the transmembrane domain by alternative splicing.[3] Similarly, BTC-δ4 induced differentiation of pancreatic β cells without stimulating proliferation of AR42J cells.[18]

Discussion

The design of IgG hinge-fused sErbB receptors successfully and efficiently formed dimeric structures that recognized and bound to BTC. The affinity of BTC-WT protein for binding to sErbB1-HF was similar to the activity of BTC and intact ErbB1 previously reported.[5] These results indicate that sErbB-HF conforms stoichiometrically active homodimers with the correct conformation that recapitulates the ECD in the membrane-bound form of the ErbB receptor as depicted in Fig. 1a. The present study demonstrates that the IgG hinge region is sufficient to construct sErbB dimers when fused to the carboxyl-terminus. Addition of different epitope tags to the hinge region that is fused to sErbB receptors should enable distinguishing the four types of ErbB receptors with epitope-specific antibodies and should not substantially inhibit ligand binding. Another advantage of this type of fusion construct is that it does not necessitate using antibodies that are specific to each type of ErbB receptor.

In the use of sErbB1 and sErbB4 constructs as probes, we screened out a mutant protein, BTC-E/88/K, from a BTC derivative expression library that was prepared by an error-prone PCR procedure. BTC-E/88/K showed significant loss of affinity for binding to ErbB1 while maintaining affinity to ErbB4.

The three-dimensional structures of the ECD of all ErbB family members have recently been determined from crystallized proteins.[19–23] ErbB1 is the only protein for which the structure has been determined as a complex with its ligands, EGF and TGF-α.[19,20] When the three-dimensional structure of TGF-α [Protein Data Bank (PDB) ID 1YUF] was compared with that of BTC (PDB ID 1IOX), E88 in BTC was found to correspond to E27 in TGF-α.[24,25] This position is marked by a dagger in Fig. 3c. The three-dimensional structure of the ErbB1–TGF-α complex (PDB ID 1MOX) shows that the anionic residue of E27 in TGF-α interacts with the cationic residue of R125 in ErbB1 through electrostatic interaction with their side chains (Fig. 7).[20] A comparable interaction between BTC and ErbB1 should also occur. By replacement of the E88 residue in BTC with the electrostatic charged K residue in the BTC-mut,

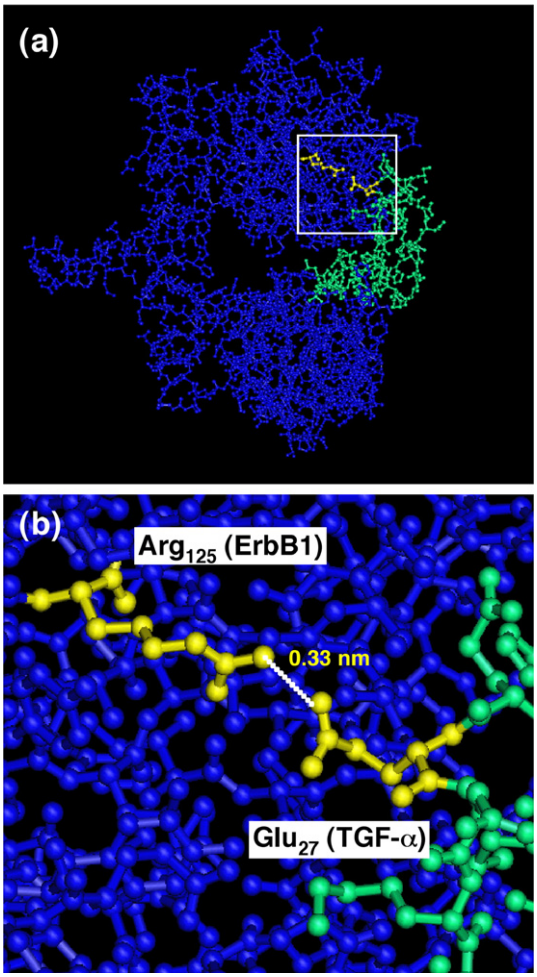

Fig. 7. Possible interaction between E27 in TGF-α and R125 in ErbB1. These schematic drawings are based on the PDB file of the crystal structure of sErbB1 and TGF-α (PDB ID 1MOX) and drawn by Cn3D (http://130.14.29.110/Structure/CN3D/cn3d.shtml). (a) Overall structure of TGF-α and ECD of the ErbB1 complex. Blue balls and sticks depict ECD of ErbB1, while light green balls and sticks depict TGF-α. (b) The interaction site is zoomed. E27 in TGF-α and R125 in ErbB1 are depicted in yellow; the white dotted line shows the distance of these two amino acid residues, estimated to be 0.33 nm with the use of the Swiss-Pdb Viewer (http://expasy.org/spdbv/).

protein interaction with the R125 residue of ErbB1 is converted to a repellant, such that the BTC-E/88/K mutant protein has a reduction in its affinity for ErbB1. In ErbB4, the amino acid residue corresponding to R125 in ErbB1 is Y123, which is neither a charged nor a polar residue.[23] This effect may explain the fact that BTC-E/88/K did not show loss of affinity to ErbB4 since the electrostatic charge of E88 in BTC should minimally participate in the interaction between BTC and ErbB4. Further screening of the mutant library should help identify the amino acid residues that are significantly responsible for regulating the affinity of binding between BTC and ErbB4 in positions other than E88.

The presence of a third and unique receptor for BTC that is distinct from any of the ErbB receptors has been suggested.[26] A novel variant of BTC that is produced by differential mRNA splicing was found in the human breast cancer cell line MCF-7.[3] The transcript of this variant was also found in normal pancreas, liver and kidney, as well as in breast tissue-derived fibroblasts. Due to the loss of exon 4, the BTC precursor is translated without the C-loop in the EGF motif and transmembrane domain from amino acid residue C95 to amino acid residue H143. Since this BTC variant does not contain the transmembrane region, the spliced protein should be secreted together with the cytoplasmic domain of the BTC precursor. This variant has been named BTC-δ4 and has been shown to have differentiation activity.[18] BTC-δ4 did not promote the growth of cells since it lacked an incomplete EGF motif, which would not be recognized by ErbB1 anymore. Also, the mutant with a deletion in the C-terminus is induced in the differentiation of AR42J cells without promoting cell growth.[27] Novel cell surface receptors that BTC, BTC-E/88/K, the BTC C-terminal deletion mutant or BTC-δ4 might bind to, that may stimulate a signal transduction pathway that is responsible for inducing the differentiation of pancreatic β cells and that might recognize only the A-loop and B-loop structures in the EGF motif may exist. There is also an additional possibility that a cluster of basic amino acid residues that reside within the cytoplasmic region of BTC such that BTC might function in a manner similar to the TAT peptide is incorporated into the cytoplasm by endocytosis when translated like the secreting form of BTC-δ4.[28] In that case, it might work itself as a transducer of differentiation signal like the cytoplasmic domain of ErbB4 or HB-EGF.[29,30]

Gene therapy using NeuroD and BTC was reported to reverse diabetes in mice.[31] In that study, the NeuroD and BTC genes were simultaneously introduced into the liver cells by a helper-dependent adenovirus and induced neogenesis of islet in the liver. This is a very intriguing finding for the future therapy of insulin-dependent diabetes. Moreover, BTC can promote the differentiation of hepatocyte stem-like cells to insulin-producing cells without exogenous NeuroD.[32] However, BTC might enhance potential tumor growth by activating ErbB1 in a manner that is similar to TGF-α when it is overexpressed and induces tumor growth.[33] Accordingly, we consider the BTC-E/88/K protein variant, which has minimal growth-promoting activity as compared with BTC-WT, as a potential candidate for use in gene therapy. Instead of using a viral expression vector, bio-nanocapsule, which is a recombinantly prepared envelope of hepatitis B virus without viral genome targeting human hepatocytes, would be the best candidate for the gene delivery vector in the case of gene therapy.[34–36] Since retargeting of modified bio-nanocapsule is possible by replacing the pre-S1 region of the L protein, which is responsible for recognizing human hepatocytes, with candidate peptides that have an affinity to target other types of cells or tissues, the BTC variant peptide that has an affinity for progenitors of pancreatic β cells would be a

possible effective delivery vector for regeneration therapy.[35] Further investigation and progress in the use of BTC-E/88/K, which fails to bind with high affinity to ErbB1 but possesses the specificity and affinity for binding to ErbB4, could show that it might also be efficacious as a delivery system to target ErbB4-overexpressing tumors, such as ependymoma and medulloblastoma.[37]

In conclusion, we have demonstrated a novel BTC-mut protein with a single point mutation replacing E88 with K. This mutant protein, BTC-E/88/K, maintains high affinity for binding to ErbB4, whereas the affinity to ErbB1 is substantially decreased. As a result, BTC-E/88/K can induce the differentiation of AR42J cells, while it showed very weak stimulation of cell growth. BTC-E/88/K would be a good candidate for diabetes therapy by regenerating pancreatic β cells *in vivo*. In this study, we have successfully shown that the dual biological activities of BTC can be completely separated by introducing a point mutation into BTC. Our future goals include the determination of the amino acid residues that are responsible for interaction of BTC with ErbB1 or ErbB4 and the development of more active BTC-muts that possess differentiation activity only, without possessing significant mitogenic activity.

Materials and Methods

Materials

Deoxy-ATP, deoxy-TTP, deoxy-CTP and deoxy-GTP were from TOYOBO (Osaka, Japan). Deoxy-ITP was from Roche (Basel, Switzerland). MTT was from Sigma-Aldrich (St. Louis, MO). Eagle's minimum essential medium (EMEM) and Dulbecco's modified Eagle's medium were from Nissui Pharmaceutical (Tokyo, Japan). rhBTC was prepared as described previously.[2] Recombinant human EGF was from PeproTech (London, England).

Construction of sErbB expression plasmids

The ECD region from amino acid residues 1–640 coded in the human ErbB1 gene (GenBank accession no. X00588) and that from amino acid residues 1–650 coded in the human ErbB4 gene (GenBank accession no. L07868) were amplified by PCR from the plasmid pCO12-EGFR (RIKEN, Wako, Japan) and from a human fetal heart cDNA (Stratagene, La Jolla, CA) with sense primers and anti-sense primers, respectively (Table 3). Both sense and anti-sense primers were designed to include appropriate restriction sequences. The PCR products were cloned into the TA cloning vector pCR2.1 (Invitrogen, Carlsbad, CA). The resultant plasmids were digested by XhoI and AgeI to excise the fragment coding for the ErbB1 ECD and by BglII and AgeI to excise the fragment coding for the ErbB4 ECD. These fragments were then inserted downstream of the cytomegalovirus promoter in the pEGFP-N1 expression vector plasmid (Stratagene) together with a synthetic oligonucleotide coding a FLAG epitope sequence (Table 2) inserted at the site digested by AgeI and NotI, yielding the expression plasmids pBO507 for sErbB1-F and pBO515 for sErbB4-F. Finally, synthetic oligonucleotide encoding for the hinge region of mouse IgG_1 heavy chain (GenBank accession no. J00453) (Table 4) was inserted into the plasmids pBO507 and pBO515 at each AgeI site, yielding plasmids pBO547 for the expression of sErbB1-HF and pBO548 for the expression of sErbB4-HF. Each DNA sequence coding for ErbB1 ECD and ErbB4 ECD was confirmed with the use of an ABI-PRISM 310 Genetic Analyzer (Applied Biosystems, Foster City, CA).

Construction of expression plasmids for tagged BTC

The expression vector for the mature form of human BTC that was tagged with His, myc and HA was constructed as follows: The synthetic oligonucleotide coding the HA peptide derived from the human influenza HA protein was inserted at the BamHI site of plasmid pET14b (Novagene, San Diego, CA), which is prepared for His-tagged recombinant expression to construct pET14b-HA. On the other hand, the DNA coding mature BTC was amplified from human mature BTC expression plasmid pBO41 by PCR using a forward primer,[2] which was designed with an NdeI site containing a methionine codon at the amino-terminal of mature BTC, D32, and a reverse primer replacing the stop codon to a leucine codon within the BamHI site. Amplified DNA was cloned into the TA cloning vector pCR2.1 and excised with NdeI and BamHI. This fragment was inserted into pET14b-HA to construct the plasmid for His–BTC–HA expression. This plasmid was further digested with NdeI, and a synthetic oligonucleotide coding a myc epitope tag (Table 4) was inserted. Finally, the expression vector for His–myc–BTC–HA under the control of T7 promoter was constructed and designated as pBO1260.

Expression and purification of sErbBs

The plasmids pBO547 and pBO548 were transfected into the human embryonic kidney cell line 293-H cells (Invitrogen) by electroporation with Gene Pulser II (Bio-Rad, Hercules, CA) to produce sErbB1-HF and sErbB4-HF, respectively. Cells were cultured in the presence of 1 mg/ml of G418 for 1 month to isolate stable cell lines expressing each sErbB-HF. Ten million 293-H cells expressing each sErbB-HF were cultured in 300 ml of Dulbecco's modified Eagle's medium containing 30 mM Hepes, pH 7.5, 5%

Table 3. Primers for amplifying ECD of ErbB

Gene name	Sequence (5′→3′)	Size of product (bp)	GenBank accession no.
ErbB1 (1–640)			
Forward	tcttcctcgagcagcgatgcgaccctccgg	1949	X00588
Reverse	ggatcaccggtccattcgttggacagcctt		
ErbB4 (1–650)			
Forward	gcacgagatctgagacttccaaaaaatgaa	1988	L07868
Reverse	caatcaccggtgttctagcatgttgtggta		

Table 4. Nucleotide linkers and deduced peptide sequences fused to ErbB or BTC

Tag	Sequence
Mouse IgG1 hinge region	
Sense (5′→3′)	ccggtgcccagggattctggttgtaagccttgcatatgtgta
Anti-sense (3′→5′)	acgggtccctaagaccaacattcggaacgtatacacatggcc
Amino acids	P V P R D S[a] G C K P C I C V
FLAG-tag	
Sense (5′→3′)	ccggtcaagctagattacaaggatgacgacgataagatttagc
Anti-sense (3′→5′)	agttcgatctaatgttcctactgctgctattctaaatcgccgg
Amino acids	P V K L D Y K D D D D K I -[b]
myc-tag	
Sense (5′→3′)	tatggagcagaaactcatctctgaagaggatcttgg
Anti-sense (3′→5′)	acctcgtctttgagtagagacttctcctagaaccat
Amino acids	M E Q K L I S E E D L G
HA-tag	
Sense (5′→3′)	gatcctacccatacgatgttccagattacgctt
Anti-sense (3′→5′)	gatgggtatgctacaaggtctaatgcgaactag
Amino acids	S Y P Y D V P D Y A -

[a] Underlined S is a replacement of the original amino acid residue C because this cysteine residue is not responsible for the heavy chain dimer formation in the immunoglobulin molecule, avoiding unexpected disulfide bond formation.
[b]"–" depicts a stop codon.

Daigo's GF21 (Nihon Pharmaceutical, Tokyo, Japan), 0.5 mg/ml of G418 and 0.05% Pluronic F-68 (SIGMA) at 37 °C for 5 days, followed by 5 days of incubation after the addition of 200 ml of fresh medium, after which the conditioned medium from the cell was collected.

The collected supernatants were passed over a 1-ml column of anti-FLAG M2 agarose affinity gel (SIGMA). The column was then washed with phosphate-buffered saline (PBS) in Dulbecco's formula, and the bound proteins were eluted with 0.1 M sodium phosphate buffer, pH 3.5. Fractions containing sErbB-HF protein were neutralized with 1/10 volume of 2 M sodium phosphate buffer, pH 8.0, and the buffer was then replaced with PBS through a desalting column PD-10 (GE Healthcare, Piscataway, NJ).

Random mutagenesis of BTC

To create a cDNA library of BTC with random point mutations, we employed an error-prone PCR procedure. Error-prone PCR was carried out on cDNA fragment coded for the EGF domain of BTC to create randomized point mutations. The reaction mixture contained 1 μM concentration of each sense primer corresponding to the upstream sequence of the EGF motif and anti-sense primer complementary to the HA-tag sequence, 0.1 mM deoxy-TTP, 0.1 mM deoxy-CTP, 0.1 mM deoxy-GTP, 10 μM deoxy-ATP, 0.1 mM deoxy-ITP, 20 mM Tris–HCl, pH 8.8, 10 mM KCl, 10 mM $(NH_4)_2SO_4$, 2 mM $MgSO_4$, 0.1% Triton X-100, 10 μM $MnCl_2$, 20 ng of pBO1260 as the template and 0.05 U/μl of a reaction of Taq DNA polymerase (New England BioLabs, Ipswich, MA). The reaction was carried out by starting at 95 °C for 5 min, followed by 25 cycles of three steps consisting of 95 °C for 30 s, 55 °C for 30 s and 72 °C for 30 s. An elongation step at 72 °C for 1 min was added at the end of the final reaction cycle. After the reaction was completed, the solution was applied onto 2% agarose gel electrophoresis and the band of amplified DNA was cut out and extracted with a QIAEX II Gel Extraction Kit (QIAGEN, Hilden, Germany). The extracted DNA fragment was then used as a primer in the following PCR reaction: One microliter of DNA solution was added to the reaction mixture containing 20 ng of pBO1260 as a template and 0.02 U/μl of PfuTurbo DNA polymerase (Stratagene). The mixture was heated to 95 °C for 2 min, and the reaction was then processed through 20 cycles of three steps of 95 °C for 1 min, 55 °C for 1 min and 68 °C for 20 min and finalized by the elongation step at 68 °C for 10 min. After the PCR reaction, the restriction enzyme DpnI was added to the reaction mixture to digest the template plasmid DNA by the incubation at 37 °C for 1 h. Finally, *E. coli* BL21-Gold(DE3) pLysS competent cells (Stratagene) were transformed with newly synthesized plasmid DNA. The colonies that were grown at 37 °C overnight on LB agar plates containing 100 μg/ml of ampicillin and 15 μg/ml of chloramphenicol were picked and suspended in 96-deep-well plates containing 0.4 ml/well of LB medium containing 100 μg/ml of ampicillin and 15 μg/ml of chloramphenicol (LB-Amp100/Cm15). Plates were shaken overnight at 37 °C by a Deep Well Maximizer MBR-022UP (TAITEC, Koshigaya, Japan) at 1500 rpm. Fifty microliters of cultured medium was then transferred to a second series of plates containing 850 μl/well of LB-Amp100/Cm15, followed by further incubation with shaking for 3 h at 37 °C. Then, 100 μl of LB-Amp100/Cm15 containing 5 mM IPTG was added to each well and cells were further incubated for 8 h at 37 °C with shaking. Cells were harvested and resuspended in 150 μl of PBS followed by freezing at −80 °C overnight. Frozen cell suspensions were thawed and sonicated for 1 min at maximum power for 20 cycles using a microplate horn equipped on an Astrason 3000 sonicator system (Misonix, Farmingdale, NY) with a 1-min interval on ice between every two cycles. Supernatants were obtained by centrifugation and stored as the crude extracts at −80 °C until they were assessed.

Purification of His–myc–BTC–HA

The procedures of bacterial cell culture and refolding recombinant BTC were basically as previously described.[2] The solution containing refolded proteins was applied to a Ni–nitrilotriacetic acid agarose (QIA-

GEN) column equilibrated with 0.1 M potassium phosphate buffer, pH 7.4, containing 0.3 M NaCl. After washing with the initial buffer containing 10 mM imidazole, the adsorbed proteins were eluted with buffer containing 150 mM imidazole. The eluted fractions were then collected and dialyzed against ultrapure water extensively. The amount of protein was estimated with BCA Protein Assay (SIGMA). The purified protein was confirmed by SDS-PAGE analysis as a single band, freeze dried and stored at −80 °C.

Western blotting

Prior to the purification of recombinant proteins, expression was confirmed by an immunological procedure as described below. Each sErbB-HF was immunoprecipitated from 1 ml of the conditioned medium with 20 μl of anti-FLAG M2 agarose by rotation at 4 °C for 16 h. The agarose beads were then washed with PBS three times and suspended in SDS-PAGE sample buffer with or without 0.4 M 2-mercaptoethanol. After electrophoresis, proteins were transferred to a polyvinylidene difluoride membrane (Bio-Rad). The proteins that were blotted onto the membrane were detected by the combination of biotin-conjugated primary antibody, anti-FLAG BioM2 antibody (SIGMA) and avidin–horseradish peroxidase (ZYMED, South San Francisco, CA). The peroxidase activity was monitored with Western Lightning Chemiluminescence Reagent Plus (Perkin-Elmer, Waltham, MA) as an enzymatic substrate by exposing on X-ray film (Fuji Film, Tokyo, Japan). The pattern on the film was densitometrically analyzed by ImageJ† for the quantification of the bands.

The lysates of bacteria transformed with each expression plasmid were electrophoresed and then transferred to polyvinylidene difluoride membranes to confirm the expression of His–myc–BTC–HA and its derivatives. The detection of protein was carried out in the same manner as in the case for the sErbB-HF, except for the biotin-conjugated primary antibody, anti-HA-biotin (Roche), alkaline phosphatase conjugates, ExtrAvidin-AP (SIGMA) and the enzymatic substrate CDP Star (New England BioLabs).

EIA

EIA was employed to assess the affinity of binding of the BTC-mut proteins to ErbB1 and ErbB4 receptors. Each well of a 96-well ELISA plate (Greiner Bio-One, Frickenhausen, Germany) was coated with 50 μl of 2-μg/ml sErbB1-HF or sErbB4-HF in PBS overnight at 4 °C, followed by incubation with 200 μl of PBS containing 0.1% bovine serum albumin (BSA) for 1 h at room temperature. After three washes with 200 μl of PBS containing 0.1% Tween-20 (PBS-T), 100 μl of the crude extracts that were diluted 30-fold in PBS containing 0.1% BSA was applied in triplicate and incubated for 1 h at room temperature. The wells were then rinsed three times with PBS-T. Fifty microliters of 1.25 mU/ml of peroxidase that was conjugated to an anti-HA high-affinity monoclonal antibody 3F10 (Roche) was added to each well and incubated for an additional 1 h. Wells were washed eight times with PBS-T, followed by incubation with 100 μl of 50 mM sodium citrate, pH 5.0, containing 0.9 mg/ml of *o*-phenylenediamine and 0.06% hydrogen peroxide (OPD solution) for 30 min. Fifty microliters of 0.5 M sulfuric acid was added to each well to quench the reaction, and the absorbance at 492 nm was measured with microplate reader MTP-120 (Corona Electric, Hitachinaka, Japan).

† http://rsb.info.nih.gov/ij/

Assessment of interaction of BTC-mut proteins with either ErbB1 or ErbB4

For the efficient screening of the BTC-mut proteins that have altered affinity for ErbB1 and/or ErbB4, the interaction index was defined. First of all, the interaction between sErbB and each BTC-mut protein was determined from EIA at 492 nm using 30-fold dilutions of crude protein extracts. The ratio of interaction for each ErbB was defined as the ratio of the value of the EIA between the BTC-mut protein and the BTC-WT. The ratios for ErbB1 and ErbB4 are defined as R1 = (A_{492} for BTC-mut)/(A_{492} for BTC-WT) when probed with sErbB1 and R4 = (A_{492} for BTC-mut)/(A_{492} for BTC-WT) when probed with sErbB4, respectively. The interaction index is defined as I = R1/R4.

Estimation of K_d value

Competition EIA was performed based on the method described by Djavadi-Ohaniance *et al.*[38] to estimate the K_d value between BTC-mut proteins and sErbB1-HF or sErbB4-HF. Each well of the plate was coated with 50 μl of 1-μg/ml BTC-WT or BTC-mut proteins with His, myc and HA tags and incubated at 4 °C, followed by blocking with 200 μl of PBS containing 0.1% BSA. Wells were then rinsed with PBS-T, and sErbB-HF with varying concentrations of rhBTC, which were premixed 30 min before, was applied to the wells. After the incubation for 30 min at room temperature, the wells were washed with PBS-T and 50 μl of 0.1-μg/ml anti-FLAG M2 peroxidase antibody was applied to each well. After an additional incubation for 1 h at room temperature, wells were washed eight times with PBS-T and incubated with 100 μl of OPD solution for 15 min. The reaction was then quenched by 0.5 M sulfuric acid, and the absorbance at 492 nm was measured.

Cell proliferation assays

Growth-promoting activity of BTC-mut proteins was evaluated by MTT assay on BALB/c 3T3 clone A31-714C4 as previously described.[2] Briefly, 2×10^3 cells were seeded in 96-well cell culture plates in EMEM containing 10% fetal bovine serum. After 20 h of incubation, the cells were made quiescent in EMEM containing 0.5% fetal bovine serum. Serially diluted growth factors were then added in triplicate, and the cells were cultured for further 48 h. At the end of this period, PBS containing 5 mg/ml of MTT was added to the final concentration of 1 mg/ml. After 6 h of incubation at 37 °C, 10% SDS containing 20 mM HCl was added to each well. MTT formazan was dissolved by overnight incubation, and the absorbance was measured at 570 nm.[39]

Differentiation and proliferation assay for AR42J cells

Differentiation of AR42JB13 B-6 36 p6 cells induced by 1 nM BTC-mut protein and 2 nM activin A was evaluated as described previously.[7] Briefly, the cells were grown and attached on cover glass slips followed by a 48-h incubation with 2 nM activin A and 1 nM BTC-WT or BTC-mut proteins. Cells were then fixed and immunostained with anti-insulin monoclonal antibody (Spring Bioscience, Fremont, CA) and tetramethylrhodamine isothiocyanate-conjugated goat anti-mouse IgG (Cappel

Laboratories, Malvern, PA). The number of insulin-positive cells was counted by epifluorescent microscopy (Olympus, Tokyo, Japan). An MTT assay was also performed on AR42J cells to investigate the growth activity of the BTC proteins overall. AR42J cells were grown and attached on cover glass slips followed by 45 h of incubation with 2 nM activin A and 1 nM BTC-WT or BTC-mut proteins. MTT solution was then added to the culture medium, and cells were incubated for further 3 h. MTT formazan was dissolved as described above, and the absorbance at 550 nm was measured.

References

1. Shing, Y., Christofori, G., Hanahan, D., Ono, Y., Sasada, R., Igarashi, K. & Folkman, J. (1993). Betacellulin: a mitogen from pancreatic β cell tumors. *Science*, **259**, 1604–1607.
2. Seno, M., Tada, H., Kosaka, M., Sasada, R., Igarashi, K., Shing, Y. *et al.* (1996). Human betacellulin, a member of the EGF family dominantly expressed in pancreas and small intestine, is fully active in a monomeric form. *Growth Factors*, **13**, 181–191.
3. Dunber, A. J. & Goddard, C. (2000). Identification of an alternatively spliced mRNA transcript of human betacellulin lacking the C-loop of the EGF motif and transmembrane domain. *Growth Factors*, **18**, 169–175.
4. Sanderson, M. P., Erickson, S. N., Gough, P. J., Garton, K. J., Wille, P. T., Raines, E. W. *et al.* (2005). ADAM10 mediates ectodomain shedding of the betacellulin precursor activated by *p*-aminophenylmercuric acetate and extracellular calcium influx. *J. Biol. Chem.* **280**, 1826–1837.
5. Watanabe, T., Shintani, A., Nakata, M., Shing, Y., Folkman, J., Igarashi, K. & Sasada, R. (1994). Recombinant human betacellulin. Molecular structure, biological activities, and receptor interaction. *J. Biol. Chem.* **269**, 9966–9973.
6. Riese 2nd, D. J., Bermingham, Y., van Raaij, T. M., Buckley, S., Plowman, G. D. & Stern, D. F. (1996). Betacellulin activates the epidermal growth factor receptor and erbB-4, and induces cellular response patterns distinct from those stimulated by epidermal growth factor or neuregulin-β. *Oncogene*, **12**, 345–353.
7. Mashima, H., Ohnishi, H., Wakabayashi, K., Mine, T., Miyagawa, J., Hanafusa, T. *et al.* (1996). Betacellulin and activin A coordinately convert amylase-secreting pancreatic AR42J cells into insulin-secreting cells. *J. Clin. Invest.* **97**, 1647–1654.
8. Li, L., Seno, M., Yamada, H. & Kojima, I. (2001). Promotion of β-cell regeneration by betacellulin in ninety percent-pancreatectomized rats. *Endocrinology*, **142**, 5379–5385.
9. Li, L., Yi, Z., Seno, M. & Kojima, I. (2004). Activin A and betacellulin: effect on regeneration of pancreatic β-cells in neonatal streptozotocin-treated rats. *Diabetes*, **53**, 608–615.
10. Li, L., Seno, M., Yamada, H. & Kojima, I. (2003). Betacellulin improves glucose metabolism by promoting conversion of intraislet precursor cells to β-cells in streptozotocin-treated mice. *Am. J. Physiol.: Endocrinol. Metab.* **285**, E577–E583.
11. Engler, D. A., Matsunami, R. K., Campion, S. R., Stringer, C. D., Stevens, A. & Niyogi, S. K. (1988). Cloning of authentic human epidermal growth factor as a bacterial secretory protein and its initial structure–function analysis by site-directed mutagenesis. *J. Biol. Chem.* **263**, 12384–12390.
12. Campion, S. R., Tadaki, D. K. & Niyogi, S. K. (1992). Evaluation of the role of electrostatic residues in human epidermal growth factor by site-directed mutagenesis and chemical modification. *J. Cell. Biochem.* **50**, 35–42.
13. Field, J. A., Reid, R. H., Rieman, D. J., Kline, T. P., Sathe, G., Greig, R. G. & Anzano, M. A. (1992). Structure–function analysis of human transforming growth factor-α by site-directed mutagenesis. *Biochem. J.* **283**, 91–98.
14. Jones, J. T., Ballinger, M. D., Pisacane, P. I., Lofgren, J. A., Fitzpatrick, V. D., Fairbrother, W. J. *et al.* (1998). Binding interaction of the heregulin-β egf domain with ErbB3 and ErbB4 receptors assessed by alanine scanning mutagenesis. *J. Biol. Chem.* **273**, 1667–1674.
15. Chamow, S. M. & Ashkenazi, A. (1996). Immunoadhesins: principles and applications. *Trends Biotechnol.* **14**, 52–60.
16. Jones, J. T., Akita, R. W. & Sliwkowski, M. X. (1999). Binding specificities and affinities of egf domains for ErbB receptors. *FEBS Lett.* **447**, 227–231.
17. Odaka, M., Kohda, D., Lax, I., Schlessinger, J. & Inagaki, F. (1997). Ligand-binding enhances the affinity of dimerization of the extracellular domain of the epidermal growth factor receptor. *J. Biochem. (Tokyo)*, **122**, 116–121.
18. Ogata, T., Dunbar, A. J., Yamamoto, Y., Tanaka, Y., Seno, M. & Kojima, I. (2005). Betacellulin-δ4, a novel differentiation factor for pancreatic β-cells, ameliorates glucose intolerance in streptozotocin-treated rats. *Endocrinology*, **146**, 4673–4681.
19. Ogiso, H., Ishitani, R., Nureki, O., Fukai, S., Yamanaka, M., Kim, J. H. *et al.* (2002). Crystal structure of the complex of human epidermal growth factor and receptor extracellular domains. *Cell*, **110**, 775–787.
20. Garrett, T. P., McKern, N. M., Lou, M., Elleman, T. C., Adams, T. E., Lovrecz, G. O. *et al.* (2002). Crystal structure of truncated epidermal growth factor receptor extracellular domain bound to transforming growth factor alpha. *Cell*, **110**, 763–773.
21. Cho, H. S., Mason, K., Ramyar, K. X., Stanley, A. M., Gabelli, S. B., Denney Jr., D. W. & Leahy, D. J. (2003). Structure of the extracellular region of HER2 alone and in complex with the Herceptin Fab. *Nature*, **421**, 756–760.
22. Cho, H. S. & Leahy, D. J. (2002). Structure of the extracellular region of HER3 reveals an interdomain tether. *Science*, **297**, 1330–1333.
23. Bouyain, S., Longo, P. A., Ferguson, K. M. & Leahy, D. J. (2005). The extracellular region of ErbB4 adopts a tethered conformation in the absence of ligand. *Proc. Natl. Acad. Sci. USA*, **102**, 15024–15029.
24. Moy, F. J., Li, Y. C., Rauenbuehler, P., Winkler, M. E., Scheraga, H. A. & Montelione, G. T. (1993). Solution structure of human type-α transforming growth factor determined by heteronuclear NMR spectroscopy and refined by energy minimization with restraints. *Biochemistry*, **32**, 7334–7353.
25. Miura, K., Doura, H., Aizawa, T., Tada, H., Seno, M., Yamada, H. & Kawano, K. (2002). Solution structure of betacellulin, a new member of EGF-family ligands. *Biochem. Biophys. Res. Commun.* **294**, 1040–1046.
26. Ishiyama, N., Kanzaki, M., Seno, M., Yamada, H., Kobayashi, I. & Kojima, I. (1998). Studies on the betacellulin receptor in pancreatic AR42J cells. *Diabetologia*, **41**, 623–628.
27. Ito, T., Kondo, M., Tanaka, Y., Kobayashi, M., Sasada, R., Igarashi, K. *et al.* (2001). Novel betacellulin

derivatives. Separation of the differentiation activity from the mitogenic activity. *J. Biol. Chem.* **276**, 40698–40703.
28. Kaplan, I. M., Wadia, J. S. & Dowdy, S. F. (2005). Cationic TAT peptide transduction domain enters cells by macropinocytosis. *J. Controlled Release*, **102**, 247–253.
29. Linggi, B. & Carpenter, G. (2006). The ErbB-4 s80 intracellular domain abrogates ETO2-dependent transcriptional repression. *J. Biol. Chem.* **281**, 25373–25380.
30. Nanba, D., Mammoto, A., Hashimoto, K. & Higashiyama, S. (2003). Proteolytic release of the carboxy-terminal fragment of proHB-EGF causes nuclear export of PLZF. *J. Cell Biol.* **163**, 489–502.
31. Kojima, H., Fujimiya, M., Matsumura, K., Younan, P., Imaeda, H., Maeda, M. & Chan, L. (2003). NeuroD–betacellulin gene therapy induces islet neogenesis in the liver and reverses diabetes in mice. *Nat. Med.* **9**, 596–603.
32. Yamada, S., Terada, K., Ueno, Y., Sugiyama, T., Seno, M. & Kojima, I. (2005). Differentiation of adult hepatic stem-like cells into pancreatic endocrine cells. *Cell Transplant.* **14**, 647–653.
33. Normanno, N., De Luca, A., Bianco, C., Strizzi, L., Mancino, M., Maiello, M. R. *et al.* (2006). Epidermal growth factor receptor (EGFR) signaling in cancer. *Gene*, **366**, 2–16.
34. Kuroda, S., Otaka, S., Miyazaki, T., Nakao, M. & Fujisawa, Y. (1992). Hepatitis B virus envelope L protein particles. Synthesis and assembly in *Saccharomyces cerevisiae*, purification and characterization. *J. Biol. Chem.* **267**, 1953–1961.
35. Yamada, T., Iwasaki, Y., Tada, H., Iwabuki, H., Chuah, M. K., VandenDriessche, T. *et al.* (2003). Nanoparticles for the delivery of genes and drugs to human hepatocytes. *Nat. Biotechnol.* **21**, 885–890.
36. Yu, D., Amano, C., Fukuda, T., Yamada, T., Kuroda, S., Tanizawa, K. *et al.* (2005). The specific delivery of proteins to human liver cells by engineered bio-nanocapsules. *FEBS J.* **272**, 3651–3660.
37. Carpenter, G. (2003). ErbB-4: mechanism of action and biology. *Exp. Cell Res.* **284**, 66–77.
38. Djavadi-Ohaniance, L., Goldberg, M. E. & Friguet, B. (1996). Measuring antibody affinity in solution. In *Antibody Engineering: A Practical Approach* (McCafferty, J., Hoogenboom, R. & Chiswell, D. J., eds), pp. 77–97, IRL Press, Oxford, UK.
39. Tada, H., Shiho, O., Kuroshima, K., Koyama, K. & Tsukamoto, K. (1986). An improved colorimetric assay for interleukin-2. *J. Immunol. Methods*, **93**, 157–165.